Systems pharmacology and blood-brain barrier functionality in Parkinson's disease
Ravenstijn, P.G.M.

Chapter 4

The Exploration of Rotenone as a Toxin for Inducing Parkinson's Disease in Rats
Application in BBB Transport and PK-PD Experiments

Paulien G.M. Ravenstijn[1], Mario Merlini[1], Marjolijn Hameetman[1], Tracey K. Murray[2], Mark A. Ward[2], Hywel Lewis[2], Gareth Ball[2], Cathy Mottart[3], Christine de Ville de Goyet[3], Thomas Lemarchand[3], Kristel van Belle[3], Michael J. O'Neill[2], Meindert Danhof[1] and Elizabeth C.M. de Lange[1*]

[1] LACDR, Division of Pharmacology, Leiden University, Leiden, The Netherlands
[2] Eli Lilly & Co Ltd, Neurodegeneration Drug Hunting Team, Windlesham, UK
[3] Lilly Development Centre S.A., Department of Drug Disposition, Mont-Saint-Guibert, Belgium

Abstract

In search for a suitable rat model to study alterations in blood-brain barrier (BBB) transport mechanisms in the course of Parkinson's disease progression, experiments were performed to characterise Parkinson's disease and safety markers following subcutaneous (SC) and intracerebral (IC) infusion of the toxin rotenone in the rat. Studies were performed using male Lewis rats. SC infusion of rotenone (3 mg/kg/day) was performed via an osmotic minipump. IC infusion of rotenone occurred directly into the right medial forebrain bundle (MFB) at three different dosages. At different times following rotenone infusion, behaviour, histopathology (tyrosine hydroxylase (TH) and α-synuclein immunocyto-chemistry), peripheral organ pathology (adrenals, heart, kidney, liver, lung, spleen and stomach) were assessed. In part of the SC and IC rats, BBB transport profiles of the permeability marker sodium fluorescein were determined using microdialysis. SC rotenone failed to produce dopaminergic lesions and led to extensive peripheral organ toxicity. BBB permeability for fluorescein following SC rotenone was changed due peripheral toxicity. In contrast, IC rotenone produced a progressive lesion of the nigrostriatal dopaminergic pathway over 28 days with no associated peripheral toxicity. IC rotenone also exhibited a large increase in amphetamine induced rotational behaviour. In addition, a few IC rats showed α-synuclein immunoreactivity and aggregation. Following IC rotenone, no changes in passive BBB permeability were detected after 14 days. SC rotenone only produced peripheral toxicity affecting BBB permeability. IC rotenone appeared to create a progressive lesion of the rat nigrostrial pathway, and may therefore be a more appropriate model of Parkinson's disease progression, compared with the most commonly used 6-OHDA rat model.

1. Introduction

Parkinson's disease is a chronic, progressive neurodegenerative disease in which nigrostratial dopaminergic neurons are gradually lost, leading to a decrease in dopamine concentration in the striatum (Dauer and Przedborski, 2003). It is the second most common neurodegenerative disease and its current therapy focuses mainly on symptomatic treatment by replacing the loss of dopamine in the striatum (Mercuri and Bernardi, 2005) by L-DOPA, the dopamine precursor. The main goal for future treatment of Parkinson's disease is the discovery and development of neuroprotective/neurotrophic drugs to diminish or, better, to halt the disease progression (Bonuccelli and Del Dotto, 2006; Chen and Le, 2006).

An important consideration for the development of neuroprotective drugs for the treatment of Parkinson's disease is the relationship between disease progression and the pharmacokinetic and pharmacodynamic (PK-PD) properties of the drug. In the PK-PD relationship of anti-Parkinsonian drugs a number of factors are of importance. One factor is transport of the drug across BBB. Drug transport between blood and the brain is governed by a number of BBB transport mechanisms as described in **Chapter 2** of this thesis.

BBB functionality is dynamically controlled by blood components and the surrounding brain cells by direct contact or indirectly by their extracellular products. Thus, BBB functionality may vary among different physiologic, pathologic, and chronic drug treatment conditions, and this may affect the BBB transport of the drug.

It is important to reveal in which direction and to what extent the different BBB transport mechanisms (and actual BBB transport of a drug) are influenced by Parkinson's disease progression. This should be adressed in a systematic manner, in relation to the physico-chemical properties of the drug. To that end preclinical studies are needed using an adequate animal model of Parkinson's disease in which Parkinson's disease progression can be identified. The most widely used animal models of Parkinson's disease are neurotoxin models with MPTP (mice, cats and primates) or 6-OHDA (mice, rats, cats and primates) (**Chapter3**, Beal, 2001). These models are generally acute (Betarbet *et al.*, 2002; Schober, 2004), but in some cases MPTP subchronic models in both primates and mice have been used (Schober, 2004). Recently, a mouse Parkinson's disease model was introduced in which MPTP was continuously administered through an osmotic minipump (Fornai *et al.*, 2005). This models appears to have the advantage over the other MPTP models that there is formation of inclusion bodies in the SNc. Although these data look very promising, it has not yet been described elsewhere.

An intrastriatal injection of 6-OHDA seems to also show a more progressive degeneration of nigral dopaminergic cells compared to intranigral injections or injections into the MFB (Sauer and Oertel, 1994; Cicchetti *et al.*, 2002). However, no Lewy body formation has yet been observed in any of the 6-OHDA models. Other approaches, which have extensively been reviewed elsewhere (Betarbet *et al.*, 2002; Uversky, 2004) include the genetic models of Parkinson's disease and the use of reserpine, methamphetamine, 3-nitrotyrosine paraquat in combination with maneb and rotenone to induce Parkinson-like symptoms. The SC infusion of rotenone to induce Parkinson's disease in the rat neurons has been reported, in

Table 1: *Setup of the experiments performed for the subcutaneous and intracerebral rotenone models. In the experiments for the subcutaneous model a 3 mg/kg/day dose of rotenone was used. In the experiments for the intracerebral rotenone model, three doses were used unless otherwise indicated: 0.5 μg, 2.0 μg and 5.0 μg.*

	frequency of measurement	Subcutaneous rotenone model				Intracerebral rotenone model			
		number of rats (n=)				number of rats (n=)			
SALINE		Day 4	Day 14	Day 21	Day 28	Day 4	Day 7	Day 14	Day 28
bodyweight	(week)daily until day of sacrifice	24	18	12	6	96	72	48	24
behaviour (Rotarod)	(week)daily until day of sacrifice	24	18	12	6		NA	NA	
histology (striatum & SNc)	once on day of sacrifice	6	6	6	6	24d	24d	24d	24d
behaviour (amphetamine challenged rotations)a	not measured for saline		NA				NA	NA	NA
BBB permeability (fluorescein)a	once on day of sacrifice		3			24d	24d	24d	24d
peripheral organ pathology	once on day of sacrifice		10a		10a	24d	24d	24d	24d
VEHICLE (DMSO/PEG)		Day 4	Day 14	Day 21	Day 28	Day 4	Day 7	Day 14	Day 28
bodyweight	(week)daily until day of sacrifice	24	18	12	6	96	72	48	24
behaviour (Rotarod)	(week)daily until day of sacrifice	24	18	12	6		NA	NA	
histology (striatum & SNc)	once on day of sacrifice	6	6	6	6	24d	24d	24d	24d
behaviour (amphetamine challenged rotations)a	once, 7 days prior to sacrifice (Day 28)		NA				8	8	
BBB permeability (fluorescein)a	once on day of sacrifice		3			24d	24d	24d	24d
peripheral organ pathology	once on day of sacrifice		10a		10a	24d	24d	24d	24d
ROTENONE		Day 4	Day 14	Day 21	Day 28	Day 4	Day 7	Day 14	Day 28
bodyweight	(week)daily until day of sacrifice	60	45	30	15	96	72	48	24
behaviour (Rotarod)	(week)daily until day of sacrifice	60	45	30	15		NA	NA	
histology (striatum & SNc)	once on day of sacrifice	15	15	15	15	24d	24d	24d	24d
behaviour (amphetamine challenged rotations)a	once, 7 days prior to sacrifice (Day 28)		NA				12c	12c	
BBB permeability (fluorescein)a	once on day of sacrifice		7			24d	24d	24d	24d
peripheral organ pathology	once on day of sacrifice		10a,b		10a,b	24d	24d	24d	24d

ahistology results on the brains of these rats are not presented in this paper, ba total of 4 rats died spontaneously during these experiments and were not included in the analysis, conly 5 μg rotenone was used in these experiments, dtotal of 24 rats used in these experiments; 8 per treatment group; NA: not applicable

which a gradual increase in striatal dopaminergic denervation with associated α-synuclein-positive cytoplasmic inclusions in nigral neurons (Betarbet *et al.*, 2000; Sherer *et al.*, 2003). Most recently, the IC infusion of rotenone into the MFB or SNc has been reported to affect the nigrostriatal pathway and produce deficits which were reversed by L-DOPA (Alam *et al.*, 2004; Antkiewicz-Michaluk *et al.*, 2004; Saravanan *et al.*, 2005; Sindhu *et al.*, 2005).

In this study, we have first investigated the influences of SC administration of rotenone (3 mg/kg/day) via an osmotic minipump in the rat on bodyweight and behaviour (locomotor activity) as measured frequently within a period of 4 weeks. Within this period, at different time intervals, rats were sacrificed and brains were used to assess nigrostriatal damage based on immunohistological staining on tyrosine hydroxylase, while in addition for all rats peripheral organ pathology was determined. In a separate experiment, at 14 days of SC administration of rotenone, BBB permeability was assessed using sodium fluorescein as a marker. In a last experiment, peripheral organ pathology was performed to determine the effect of 3 mg/kg/day rotenone systemically. In a subsequent series of experiments, the influence of IC administration of rotenone in the MFB at three different doses of rotenone (0.5, 2.0 and 5.0 μg) on nigrostriatal damage (immunohistological staining on tyrosine hydroxylase) was determined. To be able to compare these results to the results obtained in the experiments using the subcutaneous rotenone model, we carefully monitored bodyweight and peripheral organ pathology was also performed on these rats. After confirming we were producing a suitable lesion we used the highest rotenone dose (5.0 μg) in behavioural experiments and in a microdialysis experiment using sodium fluorescein as a BBB permeability marker. A summary of all the experiments which are presented in this paper is shown in Table 1.

2. Materials and Methods

Statement on use and care of animals

The experiments described in this paper were approved by the Ethical Committee on Animal Experimentation of the University of Leiden (DEC numbers 118 and 5069). For all experiments (Table 1) inbred adult male Lewis rats (250-300 g, Charles River BV, Maastricht, The Netherlands) were used. The rats were housed in standard plastic cages (six per cage before surgery and individually after surgery) with a normal 12-hour day/night schedule (lights on 7:30 AM) and a temperature of 21°C. The animals had access to standard laboratory chow (RMH-TM; Hope Farms, Woerden, The Netherlands) and acidified water ad libitum.

Surgical methods

Placement of osmotic minipumps

In these experiments, the rats were inplanted with an Alzet osmotic minipump (2ML-4, Alzet CR, Maastricht, The Netherlands) placed subcutaneously on the back of the rat. For the rats in the microdialysis experiment, the pump was placed 7 days after microdialysis surgery. The osmotic minipump was filled with either 3mg/kg/day Rotenone (Pestanal®, Sigma Alldrich BV, Zwijndrecht, the Netherlands) dissolved in a 1:1-mixture of dimethylsulfoxide (DMSO, Sigma Alldrich BV, Zwijndrecht, the Netherlands) with polyethylene glycol (PEG 200, Sigma Alldrich BV, Zwijndrecht, the Netherlands) as the vehicle (DMSO:PEG; 1:1), or filled with the vehicle alone or saline (0.9% NaCl).

Pumps were incubated in sterile saline at 37 °C overnight. For the implantation, rats were deeply anesthetised using isoflurane (Forene®, Abbott B.V., Hoofddorp, The Netherlands). The Alzet osmotic minipumps were implanted under the skin on the back of the rat. The rats were weighed on regular basis to monitor general well-being. Rats were euthanised either after 7, 14, 21 or 28 days or after the development of hunched posture suggestive of abdominal pain and upon inadequate feeding or grooming, suggestive of ongoing toxicity.

Implantation of blood cannulas

The surgery for the microdialysis study was performed under anesthesia with an intramuscular injection of 0.1 mg/kg medetomidine hydrochloride (Domitor 1 mg/ml, Pfizer, Capelle a/d IJssel, The Netherlands) and 1 mg/kg ketamine base (Ketalar 50 mg/ml, Parke-Davis, Hoofddorp, The Netherlands). Two indwelling cannulae (pyrogen-free, nonsterile polyethylene tubing, Portex Limited) were implanted, one in the left femoral artery and one in the left femoral vein. The

cannula in the left femoral vein was used for administration of fluorescein, whereas the cannula in the left femoral artery was used for serial collection of arterial blood samples. The cannulae were tunneled subcutaneously and fixed at the back of the neck with a rubber ring. The skin in the neck was stitched with normal sutures. The skin in the groin was closed with wound clips.

To prevent clotting and cannula obstruction, the cannulae were filled with a 25% (w/v) polyvinylpyrrolidone solution (PVP; Brocacef, Maarssen, The Netherlands) in pyrogen-free physiological saline (B. Braun Melsungen AG, Melsungen, Germany) containing 20 IU/ml heparin (Hospital Pharmacy, Leiden University Medical Center, Leiden, The Netherlands). After the implantation of the cannulae, the rats were placed in a stereotaxic frame and the skull was exposed for brain surgery.

Microdialysis surgery for the subcutaneous model

After the implantation of the cannulas, a small hole was drilled to allow the implantation of a microdialysis guide cannula (CMA/12, Aurora Borealis Control B.V. Schoonebeek, The Netherlands) in the striatum (relative to bregma (Paxinos *et al.*, 1985): AP: +0.4; L: +3.2; V: -3.5). Two support screws were placed to hold the guide, which was glued to the skull with dental acrylic cement (Howmedia simplex rapid + methylacrylate, Drijfhout, Amsterdam, The Netherlands). The osmotic minipump was placed 7 days after the microdialysis surgery and the experiment was carried out 14 days after pump implantation.

Microdialysis surgery for the intracerebral model

After the implantation of the cannulas, the rats received a unilateral infusion into the right MFB (AP: -2.8; L: +2.0; V: -9.0 relative to bregma; (Paxinos *et al.*, 1985)) at a rate of 0.1 µl/min for 30 minutes of either vehicle (DMSO/PEG, 1:1; n=8; referred to as sham) or 5.0 µg of rotenone (n=12). After the infusion, the needle was kept in place for another 5 minutes to allow diffusion of the fluid without leakage along the track of the needle. Subsequently, two small holes were drilled into the skull to allow implantation of a microdialysis guide cannula (CMA/12, Aurora Borealis Control B.V. Schoonebeek, The Netherlands) in the left and in the right striatum relative to bregma (AP: +0.4; L: +/-3.2; V: -3.5, relative to bregma; (Paxinos *et al.*, 1985)).

One support screw was placed as an extra anchor for fixation of the guide, which was glued to the skull with dental acrylic cement (Howmedia simplex rapid + methylacrylate, Drijfhout, Amsterdam, The Netherlands). The microdialysis

experiment was carried out 14 days after microdialysis surgery.

Experimental methods

Subcutaneous model: Behavioural experiment

For this study (in total n=108), the rats received an Alzet osmotic minipump filled with either rotenone in vehicle (n=60, for a dose of 3mg/kg/day), vehicle alone (n=24), or saline (n=24). For each treatment, the rats were divided into 4 groups with different treatment durations of respectively 4, 14, 21 and 28 days after which the rats were given an overdose of Nembutal® (Natriumpentobarbital 60 mg/ml, Ceva Sante Animale, Naaldwijk, The Netherlands) and the thorax was opened and the rat was perfused with 30 ml of saline followed by 30 ml of 10% phosphate buffered formalin (pH=7.0) via the left ventricle of the heart. Brains were removed for histopathology. During the entire course of the experiment, the bodyweight of the rats was monitored daily from Monday to Friday (Table 1). Before implantation of the minipump, the rats were trained daily for two weeks on the Rotarod (Ugo Basile, Comerio, Italy). After implantation, the rats' ability to stay on the Rotarod was tested on a daily basis during the week, in two sessions. Before the first session the rat was weighed, and then placed on the drum of the Rotarod with the head facing in the direction opposite to the direction of rotation. This forced the rat to move forward in order to stay on the rotating drum. The drum was started at a speed of 2 rotations per minute (r.p.m) and accelerated every 30 seconds to a final maximum speed of 20 r.p.m. after 5 minutes. At this time, the session was ended and the rat was allowed to recover for a 30 minute period before the second session was started. As a behavioural read-out, the time that the rat was able to stay on the drum was recorded. All rats that were unable to remain on the Rotarod for at least 250 seconds before the start of the treatment were excluded from data analysis.

Intracerebral model: Behavioural experiment

For this study, male Lewis rats received a unilateral infusion into the MFB of either DMSO/PEG (1:1; n=8; vehicle) or 5.0 µg of rotenone (n=12). Approximately 21 days after rotenone infusion the animals were placed in automated rotometers (Med. Associates Ltd.). The apparatus consisted of perspex bowls where each rat was linked to a harness carrying an infrared sensor at the top connected to a computer with ROTORAT software. The animals were tested for rotations in absence (baseline) and in the presence (stimulation) of amphetamine (5 mg/kg i.p.) to evaluate the effects of rotenone treatment on stimulant-induced rotations.

On the day of sacrifice (day 28), the animals were given an overdose of anaesthetic and the thorax was opened and perfused with 30 ml of saline followed by 30 ml of 10% phosphate buffered formalin (pH 7.0) via the left ventricle of the heart. Brains were removed for histopathology.

Microdialysis experiment

At 18-24 hours prior to the experiment, the microdialysis probes (CMA12, membrane length of 4.0 mm; Aurora Borealis Control B.V. Schoonebeek, the Netherlands) were gently inserted into the guide cannulas after removal of the probe dummies.

The microdialysis experiment was started between 7:00 and 8:00 a.m. The inlets of both microdialysis probes were connected by FEP tubing (fluorinated ethylene propylene tubing; internal volume of 1.2 µL/100 mm length; Aurora Borealis Control B.V. Schoonebeek, the Netherlands) to syringe pumps (Beehive, Bas Technicol, Congleton, United Kingdom). The probes were perfused with aECF (composition in mM: NaCl 145; KCl 2.7; CaCl2 1.2; MgCl2 1.0; ascorbic acid 0.2 in a 2 mM phosphate buffer pH 7.4 (Moghaddam and Bunney, 1989) at a flow rate of 2 µl/min. The outlets consisted of fused silica tubing (I.D. 150 µm, O.D. 375 µm; Composite Metal Services Ltd, Iikley, United Kingdom) and were connected to a microsample collector (Univentor 820; Antec, Leiden, The Netherlands), in which the samples were collected and cooled (4°C). After a stabilisation period of 60 minutes, the *in vivo* recovery of fluorescein was determined by the retrodialysis method. For this purpose, the probes were first perfused with a fluorescein solution (10 or 20 ng/ml in aECF) for 60 minutes to collect 6 fractions. The relative loss of fluorescein was calculated as an average of this period. After this period, the syringes were switched to blank aECF for the washout phase of 90 minutes. After the washout period, the intravenous administration of fluorescein was started. The venous cannula was connected to a syringe containing fluorescein (Sigma Alldrich BV, Zwijndrecht, the Netherlands) in saline (0.9% NaCl). For a dose of 6 mg/kg of fluorescein, a 2-minute intravenous infusion was started at a rate of 50 µl/min. In the first 120 minutes of the experiment, microdialysis fractions were collected at 10-minute intervals and from 120-180 minutes and from 180-240 minutes at 20- and 30-minute intervals, respectively. Blood samples (50 µl in heparinised Eppendorf vials) were taken at 0, 0.5, 2, 4, 6, 8, 10, 15, 20, 25, 30, 45, 60, 90, 120, 180 and 240 minutes after start of the fluorescein infusion. The blood samples were centrifuged for 10 minutes at 5000 r.p.m. and the plasma was pipetted into Eppendorf vials. All samples were stored at -20 C.

Histopathology

TH immunohistochemistry was performed to quantify the degree of dopaminergic neurodegeneration. In short, the brains were cut twice into 6-mm segments using a rodent brain matrix, processed, and embedded in paraffin wax. Coronal sections (8 μm) were cut through the striatum (at 1.2 mm caudal to bregma) and the SNc (from -4.5 to -6.2 mm caudal to bregma) (Paxinos *et al.*, 1985) with a sledge microtome (Microm, Walldorf, Germany). The sections were deparaffinised and rehydrated and endogenous peroxidase was quenched with 0.3% H_2O_2 for 30 min. The slides were placed in pepsin (0.2 g of Sigma-p-7000 pepsin in 50 ml of 0.01 M HCl) for 30 min, washed, and non-specific binding was blocked with 1.5% normal goat serum (Vectastain rabbit IgG ABC kit; Vector Laboratories, Burlingame, CA). This was followed by the application of the primary rabbit polyclonal anti-tyrosine hydroxylase antibody (AB152 incubated for 18 h at room temperature; Chemicon International, Temecula, CA), the secondary biotinylated antibody (Vectastain rabbit IgG ABC kit for 30 min) and the horseradish peroxidase conjugate (Vectastain rabbit IgG ABC kit for 30 min). Visualisation was carried out using 3,3'-diaminobenzidine (Vector SK-4100 Vector Laboratories, Burlingame, CA) as a chromogen. The slides were coverslipped using DPX mountant. Adjacent nigral sections were immunostained for α-synuclein using an anti-α-synuclein (1:200, AB15530, Abcam, UK).

After staining, striatal sections were scanned using SprintScan 35 with PathScan Enabler™ at a resolution of 1012 dpi. Optimas 5.2 software was used to measure the optical density of manually-defined areas of each black and white image produced as a mean grey value (MGV). TH-IR was measured for the slide (background), cortex (control tissue staining), corpus callosum (control non-cellular staining), dorsal striatum (caudate putamen, CPu) and ventral striatum (nucleus accumbens, NAcc). The values were adjusted for non-specific staining by subtracting the MGV of the corpus callosum or cortex, an area that should have no specific TH-staining. Values obtained were entered into a spreadsheet sorted by treatment group, and the mean, standard deviation and standard error (sem) calculated using formulas. These means and errors were subsequently plotted and unless otherwise stated, all striatal TH-IR values are corrected for cortical TH-IR. A series of sections through the SN (-4.5 mm -6.2 mm) were evaluated and stained. After careful evaluation under the microcope the TH-positive cells within the SNc were counted at one selected stereotaxic level (-5.2 to 5.4 mm caudal to bregma) in both vehicle treated and the rotenone-lesioned animals. The

cells were counted manually using a digital camera (Hitachi HV-C20A) attached to a light microscope (LEICA DMLB, Leica Microsystem Wetzlar GmbH) at ×20 magnification and the lesioned side is expressed as a percentage of the intact side. Light microscopy was also used to provide a qualitative assessment of the presence of α-synuclein in the SNc in the intracerebral experiment.

Peripheral organ pathology

The pathological evaluation of the brain and peripheral organs of the subcutaneous experiment was performed on 56 rats and of the intracerebral experiment on 96 rats (Table 1). After 7, 14, 21 or 28 days of treatment (for the subcutaneous experiment only 14 or 28 days), the animals were given an overdose of Nembutal® (Natriumpentobarbital 60 mg/ml, Ceva Sante Animale, Naaldwijk, The Netherlands) and the thorax was opened and the rat was perfused with 30 ml of saline followed by 30 ml of 10% phosphate buffered formalin (pH=7.0) via the left ventricle of the heart. Adrenals, heart, kidney, liver, lung, spleen and stomach were removed and immersed in 10% neutral buffered formalin (pH=7.0), trimmed after adequate fixation according to a standard operating procedure inspired from the Registry of Industrial Toxicology Animal-data (RITA) standards (Bahnemann *et al.*, 1995), and appropriate samples routinely processed to tissue blocks embedded with paraffin wax. Tissue sections were cut at approximately 3 µm, stained with Harris' hematoxylin and eosin (HE), Oil red O for neutral fat and Von Kossa's stain for mineral/calcium deposits and examined by light microscopy for relevant changes by a pathologist, without knowledge of the treatment status.

Analysis of Fluorescein

The plasma and microdialysate samples obtained in the subctaneous model experiment were analysed for fluorescein concentrations by HPLC with fluorescence detection. The HPLC system comprised a PSS Suprema size exclusion column (8x300 mm, 10 µm particle size), with a mobile phase of 0.05 M ammoniumacetate (pH=9.0) and acetonitrile (4:1 v/v). The flow rate was maintained at a flow of 1.5 ml/min. The detection was performed using a fluorescence detector (LC240, Perkin Elmer, United Kingdom) with the excitation wavelength set at 488 nm and the emission wavelength set at 512 nm. The microdialysate samples (15 µl) were injected directly onto the HPLC column. For the analysis of the plasma samples, 10 µl of plasma was added to 990 µl of an icecold artificial extracellular fluid (described above) and vortexed for 10 seconds. A 50 µl aliquot of this mixture was injected directly onto the HPLC system

equipped with a refill guard column (2 mm I.D. x 20 mm) (Upchurch Scientific, Oak Harbor, WA, USA) packed with C18 (particle size 20-40 μm) (Alltech, Breda, The Netherlands).

For the analysis of fluorescein in plasma and microdialysate samples from the intracerebral experiment, we developed an assay using the Fluostar Optima, which was a fast and reliable method. The results of the validation of this assay are presented in Table 2. The detection limit was 0.08 ng/ml. For the analysis of the microdialysate samples, 10 μl microdialysate was pipetted onto a black 96-well plate (FIA-plate flat bottom/medium binding, Greiner, Alphen a/d Rijn, The Netherlands) and 40 μl of a 0.25 M NaOH solution was added. For the analysis of the plasma samples, an aliquot of 10 μl plasma was pipetted onto a black 96-well plate and 90 μl of a 0.1 M NaOH solution was added. The fluorescence intensity was measured on the Fluostar Optima (BMG Labtech, Offenburg, Germany) at the emission wavelength of 530 nm and the excitation wavelength of 480 nm.

Table 2: *Validation of the determination of fluorescein: intra-assay and inter-assay variability, coefficients of variability and accuracy*

Compound	Added	Intra-assay (n=4)			Inter-assay (n=10)		
		Found (mean ± SEM)	CV	Accuracy	Found (mean ± SEM)	CV	Accuracy
	(ng/mL)	(ng/mL)	(%)	(%)	(ng/mL)	(%)	(%)
Fluorescein	1.0	0.9 ± 0.03	6.0	93.7	1.1 ± 0.08	22.3	107.0
	2.0	2.0 ± 0.02	1.6	98.8	2.0 ± 0.03	4.6	102.1
	5.0	5.1 ± 0.03	1.1	101.7	4.9 ± 0.07	4.4	97.5
	10.0	10.1 ± 0.08	1.7	101.3	10.3 ± 0.22	6.9	102.7

Statistical analysis

All data were statistically evaluated for significance by one-way analysis of variance (ANOVA) and a Tukey-Kramer multiple comparison test except for the microdialysis fluorescein data from the subcutaneous experiment which were evaluated using Student's t-test due to the small sample size of the saline and vehicle groups. Values of $P<0.05$ were considered significant.

3. Results

Subcutaneous model: bodyweight and locomotor activity

The subcutaneous infusion of rotenone produced a time-related reduction ($P<0.001$) in bodyweight of rotenone treated rats, compared with vehicle- or saline-treated rats (Figure 1). This reduction was most pronounced in the first 10-14 days following the start of the treatment. Behavioural analysis using the Rotarod was performed at various time points after infusion of saline, vehicle or rotenone (Figure 2A). The analysis was based on the time-period in which the rat was able to remain on the Rotarod (latency time). Results were categorised into 3 panels; panel 1 for latency times ranging between 0 and 100 sec, for panel 2 between 100 and 200 sec, and for panel 3 between 200 and 300 sec. In saline-treated rats and vehicle-treated rats only 2-3% of the animals had a Rotarod latency lower than 100 seconds whereas in rotenone-treated rats this number had increased to 30% (panels A1, B1, C1). Also, 77% of the saline-treated rats and 86% of the vehicle treated rats were able to stay on the apparatus for more than 200
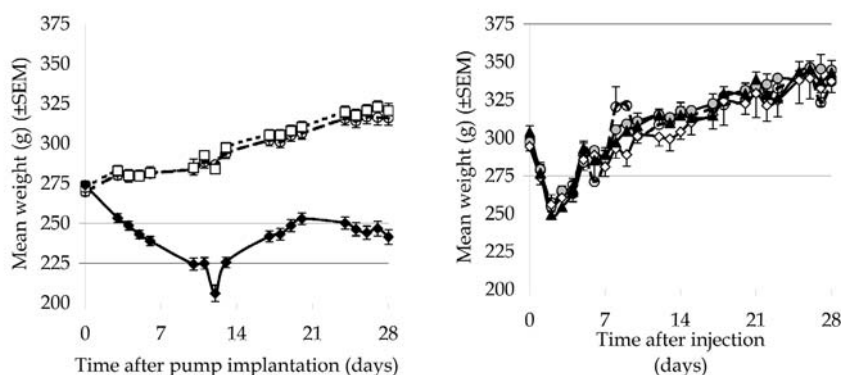

Figure 1: (LEFT panel) The effect of the subcutaneous infusion of (o) saline, (□) vehicle (DMSO/PEG) and (•) 3.0 mg/kg/day rotenone on bodyweight over time. The data are expressed as mean values ±SEM. Statistical analysis (one-way ANOVA) showed no significant difference in weight between all treatment groups on day 0 ($P>0.05$) and no significant change between the saline and vehicle groups for any time point ($P>0.05$). Significant differences were observed between the rotenone treated group and the saline treated group ($P<0.001$) or vehicle treated group ($P<0.001$) for all time points. (RIGHT panel) The effect of an intracerebral infusion of (o) artificial ECF, (• light grey) 0.5 μg rotenone, (◊) 2.0 μg rotenone or (▲) 5.0 μg rotenone (n=24) on the bodyweight over time. The data are mean values±SEM. Statistical analysis (one-way ANOVA) showed no significant difference between all groups.
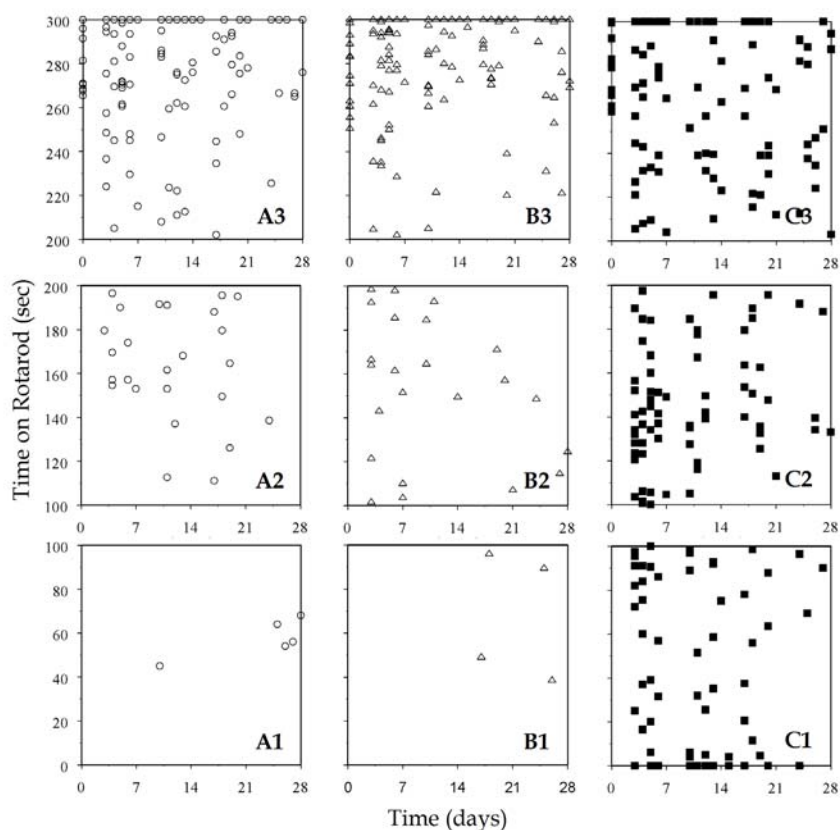
Figure 2A: Behaviour in the subcutaneous rotenone model: The time that a rat was able to remain walking on the Rotarod at different days following implantation of the osmotic minipump in (o) saline treated rats, (△) vehicle (DMSO/PEG)-treated rats, (■) 3.0 mg/kg/day rotenone-treated rats. Panels A1-C1 represent the amount of data points in the 0-100 seconds region. Panels A2-C2 represent the amount of data points in the 100-200 seconds region. Panels A3-C3 respresent the amount of data points in the 200-300 second region.

seconds, but only 45% of the rotenone-treated rats were able to stay on the Rotarod for that period of time (panels A3, B3, C3). Therefore, rotenone-treatment impaired Rotarod performance, with a greater percentage of these animals falling off the apparatus at early time points and fewer animals staying on for the full testing period (300 seconds).

Intracerebral model: bodyweight and rotational behaviour

The effect of the intracerebral infusion of either aECF, 0.5 µg rotenone, 2.0 µg rotenone or 5.0 µg rotenone into the MFB on the bodyweight of the rat (Figure 1) indicated that was a decrease in bodyweight of about 10-15% in all treatment groups in the first 2 days after surgery. However, from 2 days onwards until the end of the experiment (day 28) the bodyweight increased as normal in all treatment groups and overall there were no statistically significant differences among the various treatment groups. In agreement with this, the experimenter's observations of the rats with regard to grooming indicated no noticeable differences among control rats and rotenone treated rats. To determine the behavioural consequences of intracerebral infusion of rotenone, we performed an experiment in which we measured amphetamine (5 mg/kg i.p.) induced rotations in rats infused with 5.0 µg of rotenone and compared these results to sham (=DMSO/PEG; 1:1) infused rats (Figure 2B). The left panel depicts the mean total rotation score and the right panel illustrates the time course of the rotations for both the sham infused rats and the rotenone infused rats. The baseline of both groups, measured before the injection of amphetamine, shows no preference of any group for a particular side. However, after the amphetamine challenge the rotenone infused had a large and significant increase in the number of ipsiversive rotations.
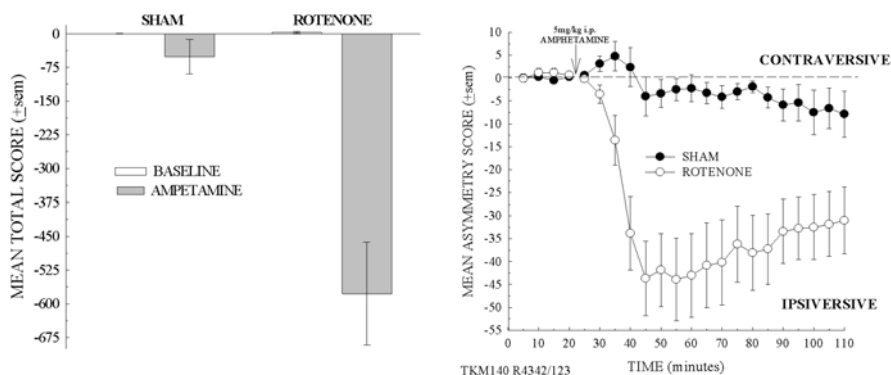

Figure 2B: Behaviour in the intracerebral rotenone model: Amphetamine (5 mg/kg i.p.) induced rotations measured on day 21 after infusion of either sham (DMSO/PEG; 1:1) or 5µg of rotenone into the MFB. Left panel depicts the mean total rotation score (±SEM) after amphetamine injection and the right panel shows the mean asymmetry score over time after amphetamine injection.

Table 3: The effect of a subcutaneous infusion of saline (n=6 per timepoint), vehicle (n=6 per timepoint) or 3 mg/kg/day of rotenone (n=15 per timepoint) on the intensity of the striatal TH-immunoreactivity. The effect of different doses of rotenone (n=8 per dose and per timepoint) and artificial ECF (n=8 per timepoint) infused into the MBF on the percentage (lesioned vs. intact brain side) striatal TH immunostaining in time.

		STRIATUM			
		4 days (MGV)	14 days (MGV)	21 days (MGV)	28 days (MGV)
Subcutaneous Rotenone model	Saline	104 ± 7	103 ± 11	85 ± 20	102 ± 11
	Vehicle	99 ± 10	98 ± 13	73 ± 11	103 ± 10
	Rotenone	88 ± 6	96 ± 7	89 ± 7	95 ± 6
		4 days (%)	7 days (%)	14 days (%)	28 days (%)
Intracerebral Rotenone model	aECF	93 ± 3	91 ± 3	96 ± 4	89 ± 3
	0.5 µg Rotenone	60 ± 12	64 ± 8	55 ± 13	64 ± 10
	2.0 µg Rotenone	50 ± 13	34 ± 15	42 ± 11	98 ± 2
	5.0 µg Rotenone	70 ± 13	44 ± 9	27 ± 9	35 ± 12

The data are presented as Mean ± SEM; MGV: Mean Gray Value

Table 4: The effect of a subcutaneous infusion of saline (n=6 per timepoint), vehicle (n=6 per timepoint) or 3 mg/kg/day of rotenone (n=15 per timepoint) on the nigral cell count. The effect of different doses of rotenone (n=8 per dose and per timepoint) and artificial ECF(n=8 per timepoint) infused into the MBF on the percentage (lesioned vs. intact brain side) nigral cell count in time.

		SUBSTANTIA NIGRA			
		4 days (cell count)	14 days (cell count)	21 days (cell count)	28 days (cell count)
Subcutaneous Rotenone model	Saline	163 ± 18	155 ± 13	204 ± 18	146 ± 8
	Vehicle	137 ± 21	136 ± 43	135 ± 38	131 ± 9
	Rotenone	129 ± 9	157 ± 17	145 ± 11	141 ± 8
		4 days (%)	7 days (%)	14 days (%)	28 days (%)
Intracerebral Rotenone model	aECF	104 ± 9	101 ± 7	84 ± 9	90 ± 5
	0.5 µg Rotenone	68 ± 15	92 ± 9	62 ± 9	62 ± 6
	2.0 µg Rotenone	72 ± 13	45 ± 12	68 ± 2	91 ± 6
	5.0 µg Rotenone	63 ± 13	74 ± 7	58 ± 6	35 ± 8

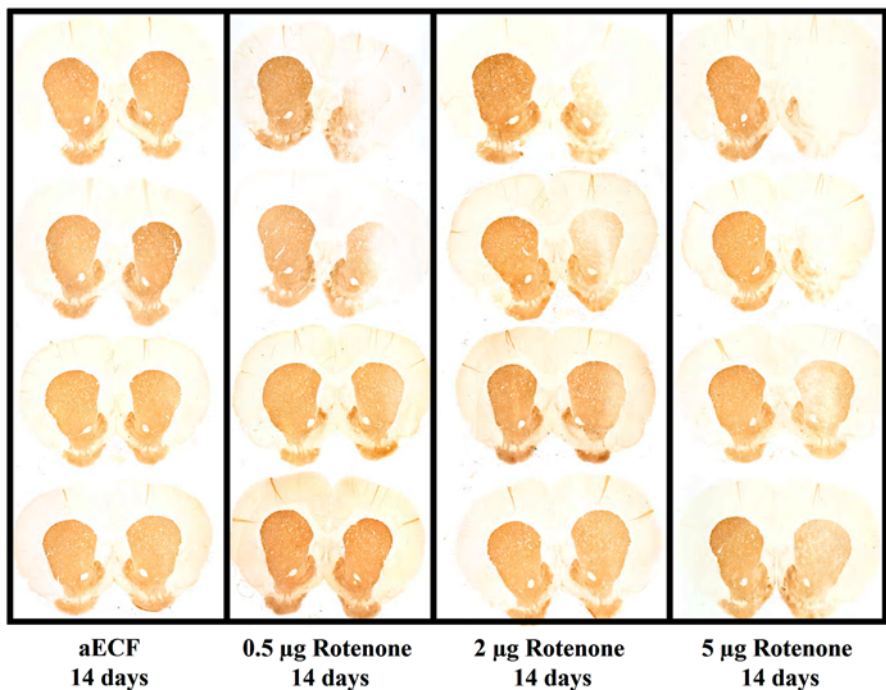The data are presented as Mean ± SEM.

Figure 3A: Intracerebral rotenone model: Images of tyrosine hydroxylase immunostaining of coronal sections taken at the level of the striatum from aECF or rotenone-infused rats (0.5, 2.0 or 5.0 μg) taken 14 days after infusion. Each treatment group is represented by 4 rats, the left striatum represents the intact side of the animal and the right striatum represents the lesioned side of the same animal. The lowest (0.5 μg) and middle (2.0 μg) rotenone doses show partial dopaminergic denervation whereas the highest rotenone dose (5.0 μg) had more pronounced loss in staining and some rats had almost complete dopaminergic denervation.

Histopathology

Subcutaneous model

Looking at the individual subcutaneous rotenone rat model data from the behavioural and microdialysis experiments, only 2% of the rotenone-treated rats showed any loss of TH staining in the striatum. The loss of striatal staining in these particular rats showed a similar pattern to that reported by Betarbet (Betarbet *et al.*, 2000). No loss of cell bodies in the SNc of any animals in the present studies was observed. The mean data for the striatum and SNc are shown in Table 3 and Table 4, respectively. No significant difference was seen in the mean striatal TH immunostaining of control, vehicle and rotenone treated rats or in the mean number of TH positive cells in the SNc among these groups.
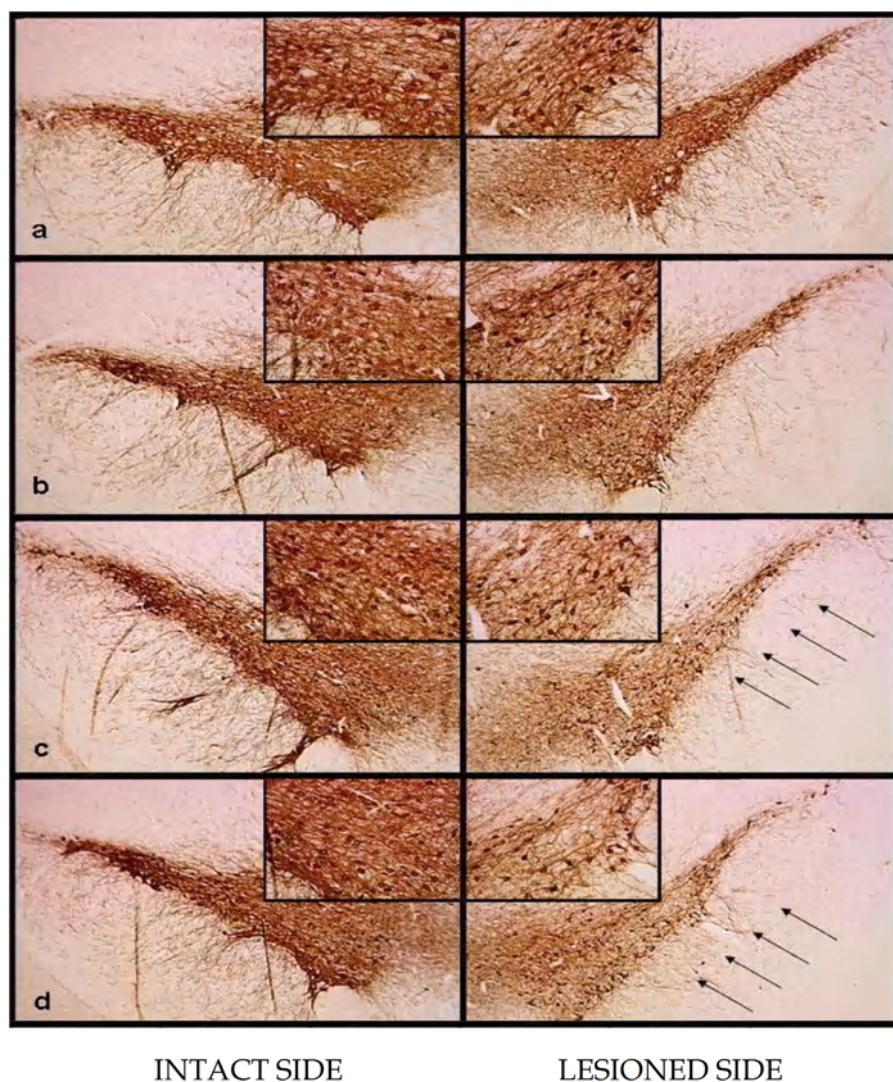
INTACT SIDE   LESIONED SIDE

Figure 3B: Intracerebral rotenone model: Images of tyrosine hydoxylase staining at the level of the substantia nigra from aECF (**a**) or rotenone-infused rats (0.5 (**b**), 2.0 (**c**) or 5.0 (**d**) µg) on day 14 after infusion. The left hand images show the intact substantia nigra with higher magnification of the cell bodies as insets. The right hand side shows the lesioned side of the brain with insets showing a higher magnification of the cell bodies. There is a clear dose dependent loss in TH positive cells and processes (see arrows) with increasing concentrations of rotenone.
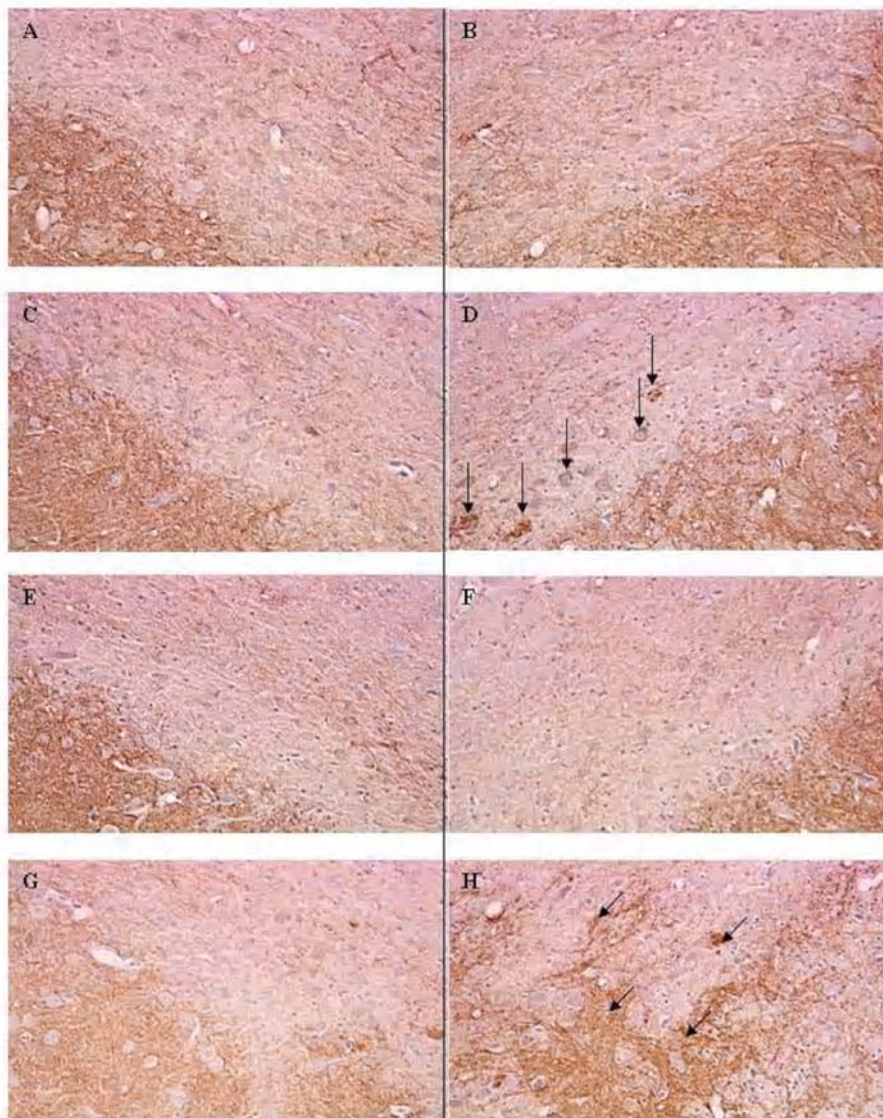
Figure 4: Intracerebral rotenone model: Examples of α-synuclein positive staining in the SNc of rats that have received 0.5 μg (C and D), 2.0 μg (E and F) or 5.0 μg (G and H) rotenone or aECF (A and B) into the left medial forebrain bundle (MFB, stereotaxic coordinates: AP: -2.8, Lat: +2.0, V: -9.0) and killed off 28 days post surgery. Both the intact SNc (A, C, E and G) and the lesioned SNc (B, D, F and H) are shown at 20x magnification. α-synuclein staining was visualised with 3-6-diaminobenzidine (DAB) with a haematoxylin counter stain.
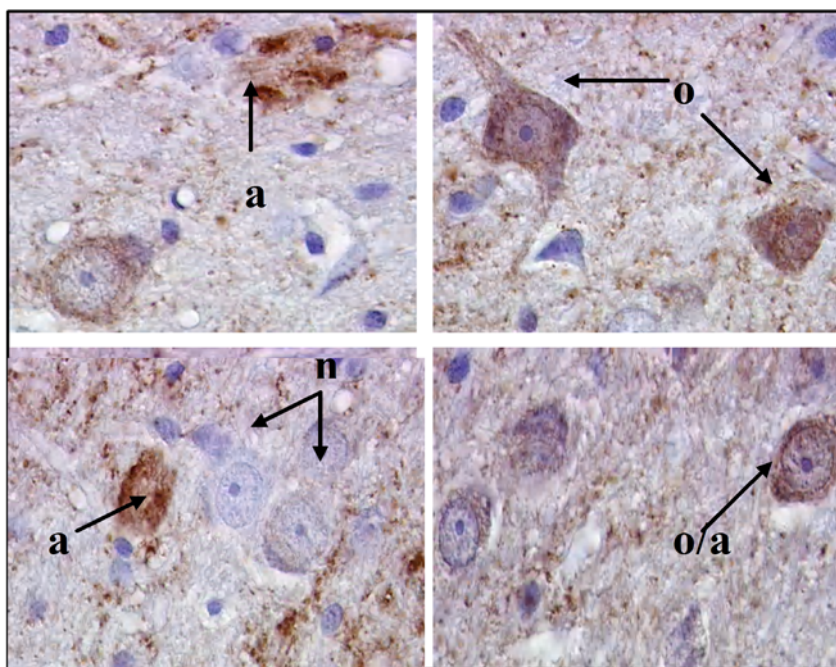
*Figure 5: Intracerebral rotenone model: Examples of possible α-synuclein overexpression (**o**) and aggregation (**a**) in dopaminergic cells compared to non-expressing cells (**n**) within the SNc of rats with rotenone-induced lesions of the MFB. Images are at 100x magnification, α-synuclein was visualised with DAB and a haematoxylin counterstain.*

Intracerebral model

The histological evaluation of the intracerebral infusion of rotenone indicated that there was no effect of the aECF infusion on the percentage of striatal TH immunostaining (Table 3 and Figure 3A), while there was a dose-dependent decrease in TH staining in rats with rotenone infusion. The dose-dependent nature of the toxin effect was most pronounced on day 14 after infusion. However, while the damage appeared to be progressive, there were no significant differences among any of the rotenone doses on day 28 compared to day 14 and a time-dependent decrease can only be observed for the 5.0 µg rotenone dose. Also, there appears to

be an increase in TH staining in both the striatum and SNc for the 2.0 µg dose between day 14 and 28. The TH immunostaining of the SNc (Table 4 and Figure 3B) showed that aECF infusion did not alter the number of TH positive nigral cells, but infusion of rotenone produced dose-dependent decrease in cell number, although less pronounced than that observed in the striatum.

The results of α-synuclein immunostaining of the SNc indicated that there were α-synuclein positive cells in a few of the rotenone treated rats (Figure 4 and Figure 5). The α-synuclein staining was variable among rats while there were more positive cells in some of the rotenone treated rats, without an increase α-synuclein staining in several others.

Peripheral organ pathology

Subcutaneous model

Four rats (20%) died spontaneously after 3-5 days of rotenone administration (3.0 mg/kg/day). No peripheral organ pathology was performed on these rats. In the surviving rats, significant treatment-related changes were observed in the stomach and minor changes were observed in the liver and heart. These changes were attributed to rotenone administration and are summarised in Table 5. Some minor changes were also seen in the liver and adrenals. The latter changes were most probably the consequence of decreased food consumption or complete anorexia and stress, respectively.

Table 5: Subcutaneous rotenone model: Incidence (%) of rotenone-related histopathological changes in Lewis rats (n=56) sacrificed on schedule.

| Scheduled Sacrifices	Day 14			Day 28			All Day Combined		
Groups	saline n=10	vehicle n=10	rotenone n=8	saline n=10	vehicle n=10	rotenone n=8	saline n=20	vehicle n=20	rotenone n=16
Stomach									
Mineralisation, minimal to moderate	0	0	2 (25%)	0	0	5 (63%)	0	0	7 (44%)
Forestomach mucosal thinning, min to slight	0	0	2 (25%)	0	0	1 (13%)	0	0	3 (19%)
Heart									
Myocardial Necrosis, minimal	0	0	2 (25%)	0	0	0	0	0	2 (13%)
Liver									
Decreased glycogen content, marked to severe	0	0	7 (88%)	0	0	5 (63%)	0	0	12 (75%)
Centrilobular Single Cell Necrosis, slight	0	0	2 (25%)	0	0	0	0	0	2 (13%)
Increased Centrilobular Inflammation, slight	0	0	1 (13%)	0	0	0	0	0	1 (6%)
Oil Red O Negative Microvacuolation, slight	0	0	1 (13%)	0	0	0	0	0	1 (6%)
Adrenal									
Mineralisation, cortex, minimal, unilateral	0	0	1 (13%)	0	0	0	0	0	1 (6%)
Increased cortical vacuolation, min to slight	0	0	2 (25%)	0	0	0	0	0	2 (13%)

Time related increase in incidence and severity of gastric mineralisation, confirmed by a Von Kossa stain, was observed in the smooth muscles fibers, the elastic connective tissue and occasionally in the glandular epithelial cells of the muscular layer, the submucosa, the muscularis mucosae and glandular crypts of the stomach (Figure 6A and Figure 6B). In the heart, minimal myofiber necrosis characterised by significant coagulative necrosis of myofibers and an inflammatory response was observed in two rotenone treated rats sacrificed on day 14 (Figure 6C). In the liver, slight increase in centrilobular single cell necrosis and/or inflammation was noted in 2 rats sacrificed on day 14, above what is usually seen in overnight fasted albino rat controls (Figure 6D). A decrease in

glycogen content was found in a majority of rats (Table 5), which was characterised by a marked decrease or an absence of clear cytoplasmic spaces without sharp outlines, a smaller size of hepatocellular trabeculae and was accompanied by centrilobular hepatocellular atrophy in the most severe cases (Figures 6E-F). Even though it is only of minor importance since it is anorexia-related, the change was clearly the most dramatic in terms of incidence and severity. In the adrenal, minimal multifocal mineralisation (calcification) was seen in the cortex of a single rat sacrificed on day 28.

Intracerebral model
For the intracerebral rotenone model, no dose or time related changes were observed in the lungs, heart, liver, stomach, spleen, kidney or adrenals of rats given up to 5.0 μg of rotenone up to 28 days, suggesting no peripheral toxicity.

*Figure 6: Subcutaneous rotenone model: **6A:** Limiting ridge of the stomach, Lewis rat given 3.0 μg/day of rotenone for 28 days. The muscularis and submucosa have extensive mineralisation (arrow). Hematoxylin and Eosin (HE) stain. Original magnification 100x. **6B:** Serial section of the change observed in figure 6A stained according to von Kossa's method for calcium precipitates (arrow). Original magnification 100x. **6C:** Right ventricular free wall of the myocardium, Lewis rat given 3.0 μg/day of rotenone for 14 days. Minimal focus of myocardial necrosis (arrowheads) and adjacent perivascular mononuclear cell infiltration. HE. Original magnification 400x. **6D:** Median lobe of the liver of a Lewis rat given 3.0 μg/day of rotenone for 14 days. Slightly increased single cell necrosis (inset) and slight inflammation (aggregates of mixed cells - arrow) are observed in numerous centrilobular areas adjacent to the central veins (CV), along with slight diffuse cytoplasmic hepatocellular vacuolation (arrowheads). Occasional focal widening of the perivenous centrilobular spaces suggests loss of centrilobular hepatocytes. HE. Original magnification 100x. **6E:** Median liver lobe from a Lewis rat given saline for 14 days. Clear cells with empty spaces (interpreted as washed-off glycogen storage) and a few vacuolation (interpreted as lipid droplets) typical of normal liver of a non-fasted rat. CV: central vein. PV: portal vein. HE. Original magnification 100x. **6F:** Median lobe of the liver of a Lewis rat given 3.0 μg/day of rotenone for 28 days. Simple severe thinning of hepatic cords due to hepatocellular atrophy, with loss of clear cytoplasm and lipid vacuoles, interpreted as loss of glycogen content, typical of rats with anorexia. HE. Original magnification 100x.*
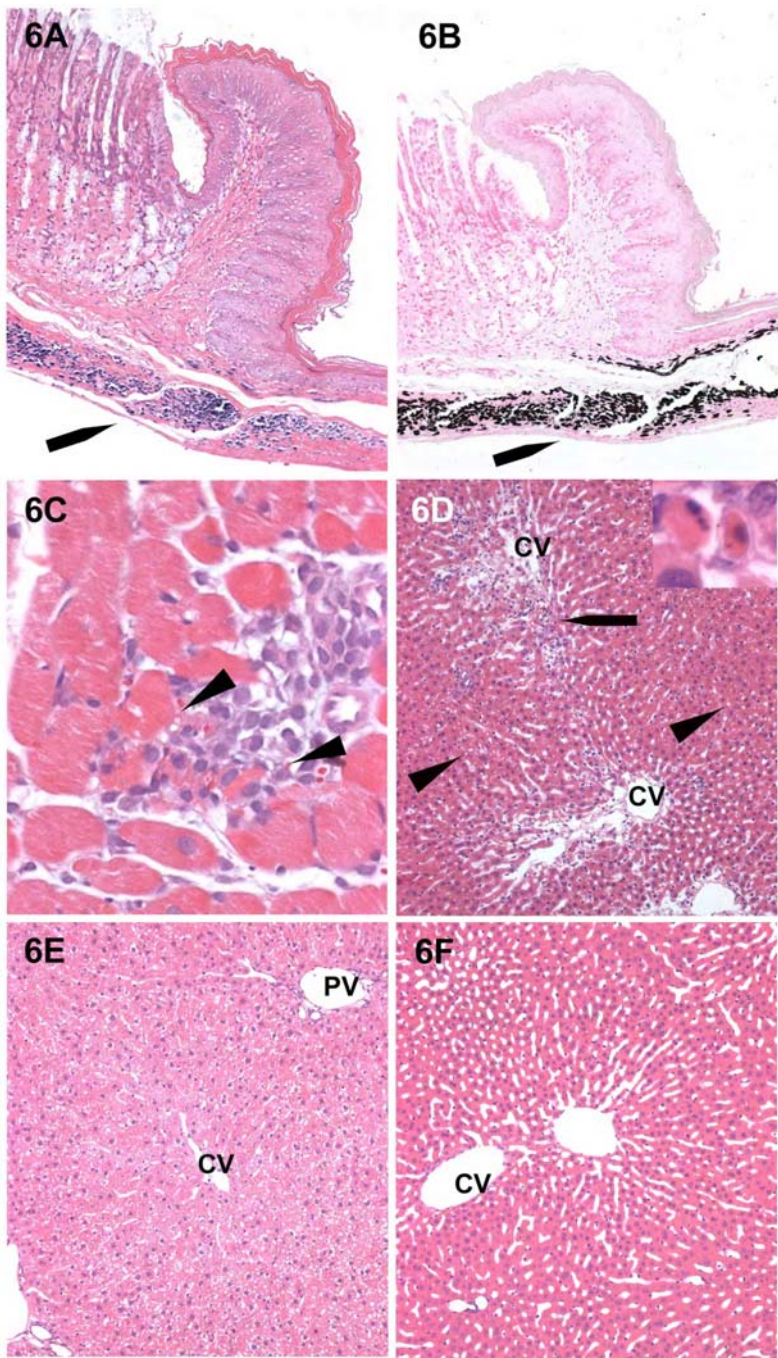
Microdialysis experiment

Subcutaneous model

For the subcutaneous rotenone model, all microdialysis concentrations were corrected for in vitro recovery (10.6 ± 0.7 %) in order to estimate brain extracellular (brain$_{ECF}$) concentrations. No statistically significant difference was found in concentration-time profiles or in area under the curves (AUC) in plasma among any of the groups indicating that the treatment with rotenone or the vehicle had no effect on the overall disposition of fluorescein (Figure 7A and Table 6). However a significant difference in the estimated brain$_{ECF}$ profiles was seen between rotenone treated rats and saline treated rats (P<0.05) and between vehicle-treated rats and saline-treated rats (P<0.01) from 80-150 minutes (Figure 8A). The BBB transport of fluorescein was calculated as the ratio of AUC$_{ECF}$ and AUC$_{plasma}$ multiplyed by 100%. The results are shown in Table 6. No statistically significant difference was seen among all treatment groups.

	AUC$_{plasma}$ (µg/ml*min) Mean ± SEM	AUC$_{ECF}$ (µg/ml*min) Mean ± SEM	AUC ratio (µg/ml*min) Mean ± SEM
Subcutaneous rotenone model			
Saline	1007 ± 200	3.0 ± 0.4	0.30 ± 0.20
Vehicle	1029 ± 117	7.1 ± 1.6	0.69 ± 1.40
Rotenone	1502 ± 306	18 ± 5	1.22 ± 1.64
Intracerebral rotenone model			
	AUC$_{plasma}$ (µg/ml*min) Mean ± SEM (%)	AUC$_{ECF}$ (µg/ml*min) Mean ± SEM (%)	AUC ratio (µg/ml*min) Mean ± SEM (%)
aECF (control)	642 ± 42	1.6 ± 0.2	0.25 ± 0.03
aECF (infused)		2.3 ± 0.7	0.36 ± 0.10
Rotenone (control)	642 ± 42	1.6 ± 0.2	0.25 ± 0.03
Rotenone (infused)		2.6 ± 1.2	0.40 ± 0.23

*Table 6: Mean area under the curves (AUC in µg/ml*min) of the plasma and estimated extracellular fluid (ECF) curves for both the subcutaneous rotenone model as well as the intracerebral rotenone model as shown in Figure 7 and Figure 8. To determine transport of fluorescein across the BBB, the AUC$_{ECF}$/AUC$_{plasma}$ ratio was calculated. The data are presented as mean values ± SEM.*

Intracerebral model

For the intracerebral rotenone model, the concentration-time profiles of fluorescein in plasma are shown in Figure 7B. All microdialysate concentrations were corrected for the average *in vivo* recovery as determined during the retrodialysis period (25 ± 1 %) in order to estimate brain$_{ECF}$ concentrations. The *in vivo* recovery was equal for the two concentrations of fluorescein used. The concentration-time profiles of fluorescein in brain$_{ECF}$ are shown in Figure 8. No significant differences were found in area under the curves (AUC) in plasma or in brain$_{ECF}$ among any of the groups indicating that the treatment with rotenone or DMSO/PEG had no effect on the overall disposition of fluorescein (Table 6). No statistical difference was observed in overall BBB transport of fluorescein among any of the groups as indicated by the AUC ratios (Table 6).
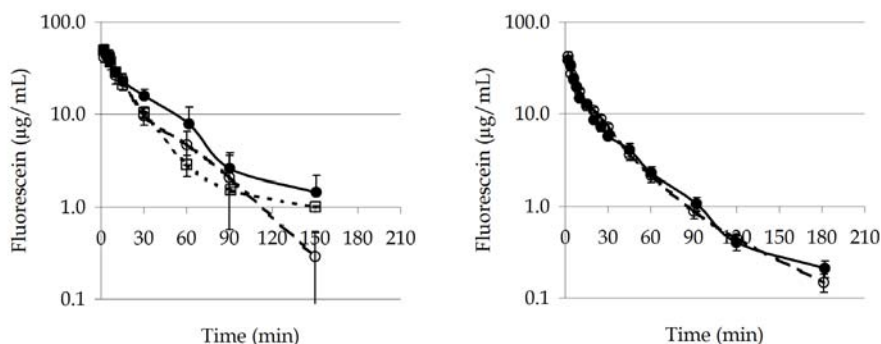

Figure 7: (Left panel) Plasma fluorescein concentration (μg/mL) vs. time (min) on day 14 after the subcutaneous infusion of (o) saline, (□) vehicle (DMSO/PEG) or (•) 3.0 mg/kg/day rotenone. The data are expressed as mean values ±SEM. (Right panel) Plasma fluorescein concentration (μg/mL) vs. time (min) on day 14 after an intracerebral infusion of (o) artificial ECF or (•) 5.0 μg rotenone. The data are mean values±SEM. Statistical analysis (one-way ANOVA) showed no significant difference between all groups for both rotenone models.
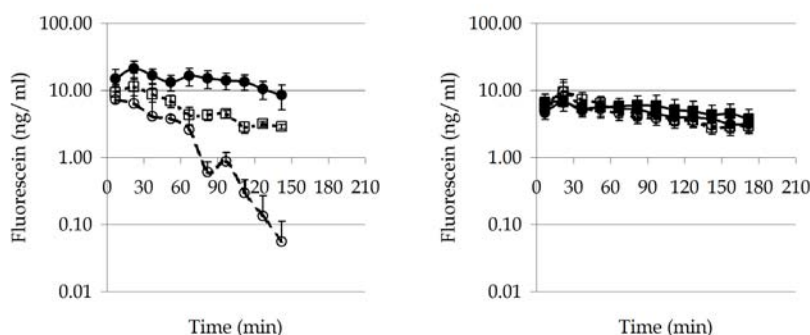
Figure 8: (Left panel) *Microdialysate fluorescein concentration (µg/mL) vs. time (min) on day 14 after the subcutaneous infusion of (○) saline, (□) vehicle (DMSO/PEG) or (●) 3.0 mg/kg/day rotenone. A significant difference was seen (time>60 min) between rotenone- and saline treated rats (P<0.05; Student's unpaired t-test) and between vehicle- saline treated rats (P<0.01; Student's unpaired t-test).*

(Right panel) *Microdialysate fluorescein concentration (µg/mL) vs. time (min) on day 14 after an intracerebral infusion of (○, □) artificial ECF or (●, ■) 5.0 µg rotenone. Circles represent the control-side of the brain and squares represent the infused side of the brain. The data are mean values±SEM. Statistical analysis (one-way ANOVA) showed no significant difference between all groups.*

4. Discussion

In this study we compared the subcutaneous and intracerebral administration of rotenone to develop a rat model for Parkinson's disease. We examined brain histology, peripheral toxicity, behaviour and BBB permeability.

Subcutaneous model

The subcutaneous infusion of rotenone resulted in minor development of dopaminergic lesions whereas profound peripheral organ toxicity was found. Although the subcutaneous infusion seemed to affect locomotor behaviour and seemed to induce an increase in BBB permeability compared to the control infusion (saline and vehicle), these results could not be correlated to nigrostriatial injury, but were most probably a consequence of peripheral organ toxicity. A time-related increase in incidence and severity of mineralisation (calcification) in the stomach was observed in rotenone-treated rats and is clearly related to the

systemic rotenone administration. Since there were no significant kidney lesions, the mineralisation is probably dystrophic secondary to cellular injury/necrosis, instead of metastatic associated with hypercalcemia or systemic Ca/P imbalance related to renal failure (uremia) (Cotran *et al.*, 1999; Palmer, 1993). However, this change would deserve further investigations to definitively rule out a metastatic mechanism. The mineralisation (calcification) in the stomach of rotenone-treated rats could be the consequence of mitochondrial injury due to inhibition of complex I and/or oxidative stress and secondary calcium influx (Sousa et al., 2003; Sousa and Castilho, 2005). The reason as to why the damaged is localised to the stomach remains unsolved. A reduced blood-flow to the stomach as a result of chronic excessive stomach distension could be an explanation, although mucosal thinning which is indicative of excessive distension was not consistently observed. This change has not been, to our knowledge, previously reported in rats that received rotenone systemically. Stomach distension is usually a non-specific change related to physiological demise, nausea (pica), severe stress or exaggerated pharmacological effect and there were no morphological evidences of atrophy of parietal cells, which could support the previously published hypothesis of achloridria with decreased wall mass (Lapointe *et al.*, 2004). The observed cardiac changes in 2 rotenone treated rats were attributed to treatment, since none were observed in any of the saline or vehicle treated rats and this change is not common in albino rats of that age; however, a background change cannot strictly be ruled out, since this change may occasionally be found in control Fischer 344 or Sprague Dawley rats (Boorman *et al.*, 1990). Liver changes were minor and related to decreased bodyweight with time and suspected decrease in food consumption. All of these changes could be secondary to the gastric lesions, especially the observed decrease in glycogen content. In addition, a few animals had atrophy of hepatocellular cords along with increased single cell necrosis, inflammation and hepatocellular microvacuolation. Although these changes could be associated with starvation, a rotenone-related effect cannot be ruled out. In contrast to a previous report with similar experimental conditions, hepatocellular coagulative necrosis was not reported in this study (Lapointe *et al.*, 2004).

The peripheral toxicity, high mortality and variability in the development of dopaminergic lesions in the brain of systemically administered rotenone as we have seen in our experiments is confirmed by literature (Betarbet *et al.*, 2000; Fleming *et al.*, 2004; Hoglinger *et al.*, 2003; Lapointe *et al.*, 2004; Sherer *et al.*, 2003; Zhu *et al.*, 2004) although it has not been so extensively investigated as in the

experiments described in this paper. In conclusion, these results indicate that the subcutaneous infusion of rotenone in the rat causes significant systemic toxicity, notably important and adverse changes in the stomach and heart, while not able to produce a sufficient amount of nigrostriatal damage as referred to as golden standard for Parkinson's disease.

Intracerebral model

The intracerebral infusion caused a progressive, dose-dependent decrease in dopaminergic neurons to about 30% in 28 days, with in a few cases α-synuclein immunoreactivity and aggregation but without any peripheral toxicity or any effect on bodyweight. Although the α-synuclein inclusions were not directly related to the severity of the dopamine lesions, they have not been observed in previous experiments using an intracerebral infusion of rotenone (Alam *et al.*, 2004; Antkiewicz-Michaluk *et al.*, 2004; Saravanan *et al.*, 2005; Sindhu *et al.*, 2005) and this result is therefore one step closer to mimicking the human pathology of Parkinson's disease. Saravan et al observed a dose-depentdent (2, 6 and 12 µg) decrease was in striatal biogenic levels already on day 5 after the infusion (Saravanan *et al.*, 2005). In our studies, we used a lower concentration range which may account for the fact that we do not see a clear dose-dependent decrease in the first 4 to 7 days. Furthermore, the decrease TH staining in time is most evident at 5.0 µg, specifically in the SNc. In the striatum the decrease seems to reach a minimal plateau after 28 days. Moreover, there appears to be an increase in TH staining in both the striatum and SNc for the 2.0 µg dose between day 14 and 28. This could perhaps be explained by the relatively low concentration infused, some rats being less susceptible to rotenone and general variability wit this toxin. Variability has also been observed in response to systemically treated rotenone rats (Betarbet *et al.*, 2000; Sherer *et al.*, 2003). It would be of interest to look at higher doses and for a longer period of time and perhaps compare different strains of rats specifically for the infusion of rotenone into the MFB. The amphetamine induced rotational behaviour of the intracerebral infused rotenone rats (5.0 µg) showed a significant preference of these rats for rotating in the ipsiversive direction on day 21 which was consistent with a unilateral lesion in the brain dopaminergic system. These results were somewhat different from a study by Sindhu *et al.* (2005) where they did not see any significant stereotypic rotations in MFB-lesioned rats (12 µg) until day 28. Again these difference may be due to variation among rat strains (Lewis rats compared to Sprague-Dawley rats).

In contrast to what would be expected on the basis of literature (Alexander *et al.*,

1994; Carvey *et al.*, 2005; Kortekaas *et al.*, 2005), no difference in BBB permeability was found in the striatum in the Parkinson's diseased brain at 14 days post-injection. It remains to be answered if changes would occur at other post-injection intervals or at other locations in the brain because microdialysis (being a good technique to study BBB transport characteristics as it monitors in time (de Lange *et al.*, 1997; Hammarlund-Udenaes *et al.*, 1997)) does not provide spatial information. In our view further investigations on BBB transport mechanisms are needed, to be performed in a strict mechanistic and quantitative manner, as a function of the disease-state.

The intracerebral administration of rotenone creates the opportunity to develop an animal model for Parkinson's disease, in which the toxin is delivered in its target brain area thereby reducing side-effects in other parts of the body that may interfere in the investigations, with features getting closer to those in Parkinson's disease patients. However, upon local delivery of the toxin, the question remains to be answered on how toxins which are capable of inducing Parkinson's disease in human are able to reach their target in the brain. Further experiments to follow the progression at longer post-injection intervals would be required to evaluate if indeed there is further disease progression and further α-synuclein development beyond 28 days. Since age seems to increase the sensitivity of dopaminergic neurons to rotenone toxicity (Phinney *et al.*, 2006), it would be worthwhile to investigate this for the IC infused rotenone rats and the influence that age might have on the development of α-synuclein inclusions.

Comparing these results to the more commonly used 6-OHDA model, in our hands, 6-OHDA infusion into the nigral cell bodies (O'Neill *et al.*, 2004) or into the MFB (Visanji *et al.*, 2006) produces a more rapid (5-10 days) loss in terminals. Also, when infused into the SNc, 6-OHDA causes an anterograde degeneration of the whole nigrostriatal dopaminergic system (O'Neill *et al.*, 2004; Sachs and Jonsson, 1975), resulting in a more rapid loss of TH positive cells. Thus, the seemingly slower effects of MFB infused rotenone obtained thusfar favours a more chronic model than 6-OHDA. This might be due to differences in the solubility, stability, and diffusion of the toxin or to the mechanism by which the toxin produces cell death. 6-OHDA can be infused into the striatum and while a rapid loss in dopamine terminals is observed, this model also produces slow progressive retrograde damage to the nigral cells (Murray *et al.*, 2003; Rosenblad *et al.*, 1999), however, so far no α-synuclein inclusions have been observed in this model. In conclusion, the data presented here indicate that rotenone infused intracerebrally is able to create a progressive rat model for Parkinson's disease.

5. Reference List

Alam M, Mayerhofer A, Schmidt WJ (2004). The neurobehavioral changes induced by bilateral rotenone lesion in medial forebrain bundle of rats are reversed by L-DOPA. *Behav. Brain Res.* 151: 117-124.

Alexander GM, Schwartzman RJ, Grothusen JR, Gordon SW (1994). Effect of plasma levels of large neutral amino acids and degree of parkinsonism on the blood-to-brain transport of levodopa in naive and MPTP parkinsonian monkeys. *Neurology* 44: 1491-1499.

Antkiewicz-Michaluk L, Wardas J, Michaluk J, Romaska I, Bojarski A, Vetulani J (2004). Protective effect of 1-methyl-1,2,3,4-tetrahydroisoquinoline against dopaminergic neurodegeneration in the extrapyramidal structures produced by intracerebral injection of rotenone. *Int. J. Neuropsychopharmacol.* 7: 155-163.

Bahnemann R, Jacobs M, Karbe E, Kaufmann W, Morawietz G, Nolte T, Rittinghausen S (1995). RITA--registry of industrial toxicology animal-data--guides for organ sampling and trimming procedures in rats. *Exp. Toxicol. Pathol.* 47: 247-266.

Beal MF (2001). Experimental models of Parkinson's disease. *Nat. Rev. Neurosci.* 2: 325-334.

Betarbet R, Sherer TB, Greenamyre JT (2002). Animal models of Parkinson's disease. *Bioessays* 24: 308-318.

Betarbet R, Sherer TB, MacKenzie G, Garcia-Osuna M, Panov AV, Greenamyre JT (2000). Chronic systemic pesticide exposure reproduces features of Parkinson's disease. *Nat. Neurosci.* 3: 1301-1306.

Bonuccelli U, Del Dotto P (2006). New pharmacologic horizons in the treatment of Parkinson disease. *Neurology 67:* S30-S38.

Boorman,G.A., Eustis, S.L., Elwell ,M.R., Mongomery,C.A. & Mackenzie,W.F. (1990). *Pathology of the Fisher Rat - Reference and Atlas.*

Carvey PM, Zhao CH, Hendey B, Lum H, Trachtenberg J, Desai BS, Snyder J, Zhu YG, Ling ZD (2005). 6-Hydroxydopamine-induced alterations in blood-brain barrier permeability. *Eur. J. Neurosci.* 22: 1158-1168.

Chen S, Le W (2006). Neuroprotective therapy in Parkinson disease. *Am. J. Ther.* 13: 445-457.

Cicchetti F, Brownell AL, Williams K, Chen YI, Livni E, Isacson O (2002). Neuroinflammation of the nigrostriatal pathway during progressive 6-OHDA dopamine degeneration in rats monitored by immunohistochemistry and PET imaging. *Eur. J. Neurosci.* 15: 991-998.

Cotran RS, Kumar V & Collins T (1999). Cellular pathology II: Adaptations, intracellular accumulations, and cell aging. In: Robbins' Pathologic basis of disease. *WB Sauners companypp* 31-49.

Dauer W, Przedborski S (2003). Parkinson's disease: mechanisms and models. *Neuron* 39: 889-909.

de Lange EC, Danhof M, de Boer AG, Breimer DD (1997). Methodological considerations of intracerebral microdialysis in pharmacokinetic studies on drug transport across the blood-brain barrier. *Brain Res. Brain Res. Rev.* 25: 27-49.

Fleming SM, Zhu C, Fernagut PO, Mehta A, DiCarlo CD, Seaman RL, Chesselet MF (2004). Behavioral and immunohistochemical effects of chronic intravenous and subcutaneous infusions of varying doses of rotenone. *Exp. Neurol.* 187: 418-429.

Fornai F, Schluter OM, Lenzi P, Gesi M, Ruffoli R, Ferrucci M, Lazzeri G, Busceti CL, Pontarelli F, Battaglia G, Pellegrini A, Nicoletti F, Ruggieri S, Paparelli A, Sudhof TC (2005). Parkinson-like syndrome induced by continuous MPTP infusion: convergent roles of the ubiquitin-proteasome system and alpha-synuclein. *Proc. Natl. Acad. Sci. U. S. A* 102: 3413-3418.

Hammarlund-Udenaes M, Paalzow LK, de Lange EC (1997). Drug equilibration across the blood-brain barrier--pharmacokinetic considerations based on the microdialysis method. *Pharm. Res.* 14: 128-134.

Hoglinger GU, Feger J, Prigent A, Michel PP, Parain K, Champy P, Ruberg M, Oertel WH, Hirsch EC (2003). Chronic systemic complex I inhibition induces a hypokinetic multisystem degeneration in rats. *J. Neurochem.* 84: 491-502.

Kortekaas R, Leenders KL, van Oostrom JCH, Vaalburg W, Bart J, Willemsen ATM, Hendrikse NH (2005). Blood-Brain Barrier dysfunction in Parkinsonian midbrain in vivo. *Ann. Neurol.* 57: 176-179.

Lapointe N, St Hilaire M, Martinoli MG, Blanchet J, Gould P, Rouillard C, Cicchetti F (2004). Rotenone induces non-specific central nervous system and systemic toxicity. FASEB J. 18: 717-719.

Mercuri NB, Bernardi G (2005). The 'magic' of L-dopa: why is it the gold standard Parkinson's disease therapy? *Trends Pharmacol. Sci.* 26: 341-344.

Moghaddam B, Bunney BS (1989). Ionic composition of microdialysis perfusing solution alters the pharmacological responsiveness and basal outflow of striatal dopamine. *J. Neurochem.* 53: 652-654.

Murray TK, Whalley K, Robinson CS, Ward MA, Hicks CA, Lodge D, Vandergriff JL, Baumbarger P, Siuda E, Gates M, Ogden AM, Skolnick P, Zimmerman DM, Nisenbaum ES, Bleakman D, O'Neill MJ (2003). LY503430, a Novel {alpha}-Amino-3-hydroxy-5-methylisoxazole-4-propionic Acid Receptor Potentiator with Functional, Neuroprotective and Neurotrophic Effects in Rodent Models of Parkinson's Disease. *J. Pharmacol. Exp. Ther.* 306: 752-762.

O'Neill MJ, Murray TK, Whalley K, Ward MA, Hicks CA, Woodhouse S, Osborne DJ, Skolnick P (2004). Neurotrophic actions of the novel AMPA receptor potentiator, LY404187, in rodent models of Parkinson's disease. *Eur. J. Pharmacol.* 486: 163-174.

Palmer N (1993). Bones and Joints. In: Pathology of domestic animals. *Academic Press Inc.pp* 1-181.

Paxinos G, Watson C, Pennisi M, Topple A (1985). Bregma, lambda and the interaural midpoint in stereotaxic surgery with rats of different sex, strain and weight. *J. Neurosci. Methods* 13: 139-143.

Phinney AL, Andringa G, Bol JG, Wolters EC, van Muiswinkel FL, van Dam AM, Drukarch B (2006). Enhanced sensitivity of dopaminergic neurons to rotenone-induced toxicity with aging. Parkinsonism. *Relat Disord.* 12: 228-238.

Rosenblad C, Kirik D, Devaux B, Moffat B, Phillips HS, Bjorklund A (1999). Protection and regeneration of nigral dopaminergic neurons by neurturin or GDNF in a partial lesion model of Parkinson's disease after administration into the striatum or the lateral ventricle. *Eur. J. Neurosci.* 11: 1554-1566.

Sachs C, Jonsson G (1975). Mechanisms of action of 6-hydroxydopamine. *Biochem. Pharmacol.* 24: 1-8.

Saravanan KS, Sindhu KM, Mohanakumar KP (2005). Acute intranigral infusion of rotenone in rats causes progressive biochemical lesions in the striatum similar to Parkinson's disease. *Brain Res.* 1049: 147-155.

Sauer H, Oertel WH (1994). Progressive degeneration of nigrostriatal dopamine neurons following intrastriatal terminal lesions with 6-hydroxydopamine: a combined retrograde tracing and immunocytochemical study in the rat. *Neuroscience* 59: 401-415.

Schober A (2004). Classic toxin-induced animal models of Parkinson's disease: 6-OHDA and MPTP. *Cell Tissue Res.* 318: 215-224.

Sherer TB, Kim JH, Betarbet R, Greenamyre JT (2003). Subcutaneous rotenone exposure causes highly selective dopaminergic degeneration and alpha-synuclein aggregation. *Exp. Neurol.* 179: 9-16.

Sindhu KM, Saravanan KS, Mohanakumar KP (2005). Behavioral differences in a rotenone-induced hemiparkinsonian rat model developed following intranigral or median forebrain bundle infusion. *Brain Res.* 1051: 25-34.

Sousa SC, Castilho RF (2005). Protective effect of melatonin on rotenone plus Ca2+-induced mitochondrial oxidative stress and PC12 cell death. *Antioxid. Redox. Signal.* 7: 1110-1116.

Sousa SC, Maciel EN, Vercesi AE, Castilho RF (2003). Ca2+-induced oxidative stress in brain mitochondria treated with the respiratory chain inhibitor rotenone. *FEBS Lett.* 543: 179-183.

Uversky VN (2004). Neurotoxicant-induced animal models of Parkinson's Disease: understanding the role of rotenone, maneb and paraquat in neurodegeneration. *Cell Tissue Res.* 318: 225-241.

Zhu C, Vourc'h P, Fernagut PO, Fleming SM, Lacan S, DiCarlo CD, Seaman RL, Chesselet MF (2004). Variable effects of chronic subcutaneous administration of rotenone on striatal histology. *J. Comp Neurol.* 478: 418-426.